A Numerical Study of Fixed Bed Reactor Modelling for Steam Methane Reforming Process

Kumar R. Rout* and Hugo A. Jakobsen

Department of Chemical Engineering, Norwegian University of Science and Technology, NTNU, N-7491, Trondheim, Norway

A numerical comparison of the pseudo-homogeneous, conventional heterogeneous, and simplified heterogeneous reactor models is performed for the steam methane reforming process. The pseudo-homogeneous reactor model consists of a set of partial differential equations, where the diffusional limitations are accounted for by considering the effectiveness factor. The heterogeneous model is divided into two categories: conventional and simplified heterogeneous models. In the conventional heterogeneous model, there are separate equations for the fluid phase species mass balance, the fluid inside the catalyst pores. This is type of reactor model is needed when there is a considerable amount of inter-phase mass transfer resistance present in the process. However, in the simplified heterogeneous reactor model the mass transport phenomenon is accounted for by accounting the efficiency factors. The model is validated against literature data. Several closures for the intra-particle mass diffusion fluxes, the Maxwell–Stefan, Wilke, dusty gas, and Wilke–Bosanquet models, have been compared on the level of the catalyst pellet and the impacts of the different particle flux closures on the reactor performance are investigated.

The simulations show that the conventional heterogeneous reactor model is necessary for the SMR process, because the effectiveness factor values of different reactions of the SMR process vary along the reactor axis. The maximum deviation between the pseudo-homogeneous and the conventional heterogeneous reactor model is less than 38 %, whereas between the conventional and simplified heterogeneous reactor models it is less than 21 %. A parametric study of the transport phenomena on the pellet level is recommended prior to any large-scale reactor simulation to determine what the rate-determining transport mechanisms are.

Keywords: steam methane reforming, pseudo-homogeneous model, conventional heterogeneous model, simplified heterogeneous model, effectiveness factor

INTRODUCTION

In the transition to sustainable energy hydrogen will play a key role as an energy carrier. Currently, hydrogen is most economically produced from fossil fuels.[1] Hydrogen as an energy carrier possesses numerous advantages over other conventional energy carriers. Hydrogen combustion provides energy based on mass basis with a lower heating value, which is 2.4, 2.8, and 4 times more than that of methane, gasoline, and coal, respectively.[2] Currently, the annual production of hydrogen is about 10^{11} kg, 98 % of which is from the reforming of fossil fuels; it is used mainly in oil refineries and ammonia and methanol production.[3] Nowadays, the emerging technology for utilization of hydrogen is the fuel cell, a rapidly emerging technology which transforms hydrogen as chemical energy into electricity. The advantages of fuel cells are that they are quiet and do not contain any hazardous material, and therefore can be considered an environmentally-friendly power source. Hence, the most studied technology for hydrogen production from fossil fuels is steam-methane reforming (SMR). Until now, this process has been the most economical commercially available method for hydrogen production.[4]

SMR reactions mainly consist of two steps. In the first step, methane reforming takes place in the presence of a Ni catalyst at elevated temperature and pressure of 500–900 °C and 3 040 kPa.[5] In second step, CO then reacts with steam to produce H_2 and CO_2 in a water gas shift (WGS) reaction.

The main reactions in the SMR process are represented by Reactions (I–III).[5]

$$CH_4(g) + H_2O(g) = CO(g) + 3H_2(g) \qquad \Delta H_{298} = 206.2\,\text{kJ/mol} \tag{I}$$

$$CO(g) + H_2O(g) = CO_2(g) + H_2(g) \qquad \Delta H_{298} = -41.5\,\text{kJ/mol} \tag{II}$$

$$CH_4(g) + 2H_2O(g) = CO_2(g) + 4H_2(g) \qquad \Delta H_{298} = 164.7\,\text{kJ/mol} \tag{III}$$

There are many key parameters in the process, including heating sources, catalyst type, operating conditions, reformer design features, and product distribution, that can influence the performance of the reforming process as noted by Armor.[11] Since it is crucial to the overall process because of its intrinsic nonlinearity and the complex phenomena involved, this manuscript focuses on the modelling and simulation of the reforming fixed bed reactor. In this paper, the performance of a industrial fixed bed tubular reactor as described by Froment and Bischoff[12] is modelled and developed.

A fixed bed reactor model for the SMR process is hard to model as it can involve many four significant dimensions: the axial and radial directions of the reactor, the catalyst particle radius, and time evolution. However, the model is usually satisfactory if axial behaviour of the reactor is well-simulated, when the research focuses principally on accuracy of different reactor models. In the chemical reactor engineering approach we desire to eliminate any

*Author to whom correspondence may be addressed.
E-mail address: kumar.rout@chemeng.ntnu.no
Can. J. Chem. Eng. 93:1222–1238, 2015

DOI 10.1002/cjce.22202
Published online 29 May 2015 in Wiley Online Library (wileyonlinelibrary.com).

mechanism that is not essential for the reactor performance from the equations to reduce the computational cost. An appropriate engineering packed bed reactor model is thus tailored for its main purpose. It is as simple as possible, but still includes a sufficient representation of the essential mechanisms involved.

The conventional classification of fixed bed reactor models contains two main categories: pseudo-homogeneous and heterogeneous models. The pseudo-homogeneous models do not account explicitly for the presence of a catalyst sorbent, in contrast to the heterogeneous models, which leads to separate equations for the fluid phase species mass balance, the fluid inside the catalyst pores, the heat transport phenomena in the solid material, and the fluid in the pores. However, the pseudo-homogeneous model requires an effectiveness factor to account for the diffusion resistance across the external film and inside the pores of the pellet. In the pseudo-homogeneous model, gradients between the solid and fluid phases are neglected and the rates are expressed in terms of the fluid-phase concentration and temperature, whereas the heterogeneous model accounts explicitly for both the phases, their heat and mass exchange, and the mass transport phenomena. The rates are expressed in terms of the solid-phase temperature and concentration profiles. Heterogeneous models are required for processes with significant temperature and concentration differences between the phases. In this study, we have divided the heterogeneous model into two different categories: conventional and simplified heterogeneous fixed bed reactor models. The conventional heterogeneous model accounts for mass transfer phenomena by considering pellet equations. In contrast, the simplified heterogeneous model contains an effectiveness factor to account for mass transport phenomena.[16,17] Both the pseudo-homogeneous and simplified heterogeneous fixed bed reactor models contain the effectiveness factor to account for internal mass transport phenomena, whereas the latter model accounts explicitly for the external heat and mass exchange to the solid phase. It will be interesting to compare the pseudo-homogeneous and simplified heterogeneous fixed bed reactor models to find the effects of heat and mass exchange to the solid phase on the overall reactor performance.

Molecular mass diffusion or molecular species transport is the movement or transport of individual molecules through a fluid by means of the random and individual movements of the molecules. Intra-particle diffusional limitations often play an important role in design of chemical reactors for gas conversion and processing. There are several models reported in the literature for multicomponent diffusion fluxes. In the Wilke model,[18,14] the binary diffusion coefficient is replaced with an effective multicomponent diffusion coefficient. This model represents a simplified version of the more rigorous Maxwell-Stefan model.[18,14,19–21] The dusty gas model[22,23] denotes an extension of the Maxwell-Stefan model in which Knudsen diffusion is considered. As an approach to calculate the combined bulk and Knudsen flux using the Fickian formulation, the Bosanquet formula is suggested in literature.[18,14,24] The approximate Wilke model is more often used in comparison to the more rigorous Maxwell-Stefan and dusty gas models in industrial reaction engineering due to their complexity and computational cost.[14]

Following established practice for heterogeneous catalytic reaction systems, the internal effectiveness factor η, with respect to the external surface conditions of the pellet, is defined by:[12,13]

$$\eta = \frac{\text{actual overall rate of reaction}}{\text{rate of reaction with surface conditions}} \quad (1)$$

The effectiveness factor depends on the size of the catalyst particles and input parameters.[8] It has been found that when increasing the size, the effectiveness factor decreases, as well as the bed pressure dropping. Generally, the particles are large enough so that the pressure drop is small, which leads to high mass transfer resistances in the particles.[10] The effectiveness factors are very low (less then 0.03) for Reactions (I–III) according to the simulation parameter reported by Elnashaie and Abashar[25] and Elnashaie et. al.,[29] which is due to high diffusional limitations in the solid porous network. If the values or the variation of the effectiveness factors throughout the reactor are known a priori, then the heterogeneous model can be reduced to a pseudo-homogeneous one[30,10] without necessitating the solution of the particle equations. However, this is not the case for the SMR reaction scheme as reported by Pantoleontos et al.[8] Treating the effectiveness factor as constant throughout the catalytic bed might lead to false estimation of the temperature and concentration profiles, because the temperature and concentration change with respect to different positions of the reactor axis and this influences the effectiveness factor values. Furthermore, the possibility of negative or asymptotic values of effectiveness factor cannot be ruled out for the SMR process.[7,25,29,31,32] Stutz et al.[33] and Parisi and Laborde[34] have studied the catalytic surface reaction for the steam methane reforming reaction. Lutz et al.[35] and Jannelli et al.[36] have investigated the steam reforming system using the thermodynamic equilibrium state. Davieau and Erickson[37] have performed studies on the reactor design for the steam reforming reaction. However, no previous research has compared the percentage of deviation between the pseudo-homogeneous, conventional, and simplified heterogeneous fixed bed reactor models for industrial cases.

Objective

The main objective of this study is to propose a comparison to investigate the type of deviation between the pseudo-homogeneous, conventional, and simplified heterogeneous fixed bed reactor models for the steam methane reforming process, in order to define a simple model as a starting point for further studies on the system identification, optimization, and control of such reactors. Next, several models for intra-particle mass diffusion fluxes, the Wilke, Maxwell-Stefan, dusty gas, and Wilke-Bosanquet models, are compared on the pellet level, and the impacts of the different flux closures on the reactor level are investigated.

MATHEMATICAL MODEL FORMULATION

Pseudo-Homogeneous Fixed Bed Reactor Model

A dynamic one-dimensional pseudo-homogenous model has been formulated for simulation of the SMR process. In this model the following assumptions are made in order to describe the fluid flow within the reactor:

1. No radial gradients in the bed; this is a valid assumption as long as the reaction scheme is not exothermic.[8] Furthermore, simulation has been performed by Lindborg[9] for the SMR process in a fixed bed reactor with different tube inner diameters, i.e. 0.1145 m, 0.2290 m, 0.3435 m, and 0.4580 m. It has been found that radial gradient increases with the increase of reactor diameter. It has been found that there is almost no radial gradient for a reactor diameter of 0.1145 m. In our simulation, the reactor inner diameter is 0.1016 m. Hence, we have neglected the radial gradient in our modelling work.

2. No side reaction occurs, such as CH_4 decomposition, Boudouard reaction, or CO reduction, to lead to carbon formation; this assumption is valid for steam to methane (S/C) ratios higher than 1.2.[38]

The general mass-balance equation for a chemical species j in reacting fluid flow with varying density, temperature, and composition is written as:

$$\frac{\partial(\epsilon_b \rho_j)}{\partial t} + \nabla .(\rho_j u_z) + \nabla .(\epsilon_b J_j) = S_j \tag{2}$$

A cross-sectional average of Equation (2) reduces the model to one dimension:[14]

$$\frac{\partial}{\partial t}\epsilon_b \langle \rho_j \rangle_{A_k} + \frac{\partial}{\partial z}\langle \rho_j u_z \rangle_{A_k} + \frac{\partial}{\partial z}\epsilon_b \langle J_{j,z} \rangle_{A_k} = \langle S_j \rangle_{A_k} \tag{3}$$

In chemical engineering practice, we drop the cross sectional averaging signs $\langle ... \rangle$ for convenience[14] and after introducing mass fractions and the transport equation for porous media flows we can write the above equation as:

$$\frac{\partial(\epsilon_b \rho_g w_j)}{\partial t} + \frac{\partial}{\partial z}(\rho_g w_j u_z) + \frac{\partial(\epsilon_b J_j)}{\partial z} = S_j \tag{4}$$

where

$$J_j = -\rho_g D_{L_j} \frac{\partial w_j}{\partial z} \tag{5}$$

The axial dispersion coefficient D_{L_j} is given by Edwards and Richardson:[39]

$$D_{L_j} = 0.73 D_{m_j} + \frac{0.5 u_z d_p}{1 + 9.49 D_{m_j}/(u_z d_p)} \tag{6}$$

The molecular diffusivities D_{m_j} of component j in the gas mixture are calculated from the Wilke equation[40] and the molecular binary diffusivities are calculated from relations by Poling et al.[41] Equation (4) is solved for the components H_2, CO, CO_2, and CH_4. H_2O is the dominating component in the system, and the mass fraction of H_2O is obtained from Equation (7):

$$w_{H_2O} = 1 - \sum_{j=1}^{5} w_j \tag{7}$$

The source term S_j in Equation (4) is a reaction source term:

$$S_j = (1 - \epsilon_b)\rho_{cat} M_j \sum_{k=1}^{3} \eta_k \mathbf{R}_k \nu_{jk} \tag{8}$$

The continuity can be obtained by adding up the species balances (4) for all the species with constraints, $\sum_{j=1}^{N} w_j = 1$ and $\sum_{j=1}^{N} J_j = 0$, which results in:

$$\epsilon_b \frac{\partial \rho_g}{\partial t} + \frac{\partial}{\partial z}(u_z \rho_g) = 0 \tag{9}$$

The cross-sectional average momentum equation for a fixed bed reactor can be given as:[46]

$$\frac{\partial(\rho_g u_z)}{\partial t} + \frac{\partial}{\partial z}\left(\frac{u_z u_z \rho_g}{\epsilon_b}\right) = \epsilon_b \frac{\partial P}{\partial z} + \epsilon_b (K_D u_z + K_V u_z^2) \tag{10}$$

However, by neglecting the left-hand part of the above equation, the pressure drop in the reactor can be calculated from Ergun's equation:[42]

$$\frac{\partial P}{\partial z} = -K_D u_z - K_V u_z^2 \tag{11}$$

where K_D and K_V are constants for the viscous and kinetic pressure drop and are given as:[42]

$$K_D = \frac{150\ \mu\ (1 - \epsilon_b)^2}{d_p^2 \epsilon_b^3} \tag{12}$$

$$K_V = \frac{1.75(1 - \epsilon_b)}{d_p \epsilon_b^3} \tag{13}$$

Solving the pseudo-homogeneous reactor model with the pressure-velocity coupling equation, i.e., Equation (10), is computationally expensive. The necessity for this model part is tested by comparing its results with the reactor model where the Ergun's equation is used to calculate the pressure profile.

An averaged one-dimensional energy equation is formulated in terms of temperature:

$$\left((1 - \epsilon_b) Cp'_p \rho_p + \epsilon_b \rho_g Cp_g\right) \frac{\partial T}{\partial t} + \rho_g Cp_g u_z \frac{\partial T}{\partial z} = -\frac{\partial}{\partial z}(Q_z) + \frac{4U}{d_t}(T_w - T) + S' \tag{14}$$

The source term (S') can be expressed as:

$$S' = (1 - \epsilon_b)\rho_{cat} \sum_{k=1}^{3} (-\Delta H_{r_k}) \eta_k \mathbf{R}_k \tag{15}$$

The heat flux Q_z can be written as:

$$Q_z = -\lambda_z \frac{\partial T}{\partial z} \tag{16}$$

The effective axial conductivity is calculated from:[43]

$$\frac{\lambda_z}{\lambda_g} = \frac{\lambda_z^0}{\lambda_g} + 0.75(Pr)(Re_p) \tag{17}$$

$$\frac{\lambda_z^0}{\lambda_g} = \epsilon_b + \frac{1 - \epsilon_b}{0.139\epsilon - 0.0339 + 2/3(\lambda_g/\lambda_p)} \tag{18}$$

The bed void fraction is calculated from a relationship given by Dixon:[44]

$$\epsilon_b = 0.4 + 0.05\frac{d_p}{d_t} + 0.412\frac{d_p}{d_t}^2 \tag{19}$$

Ideal gas law has been used to calculate mixture density:

$$\rho_g = \frac{P M_w}{RT} \tag{20}$$

Conventional Heterogeneous Fixed Bed Reactor Model

A one-dimensional dynamic conventional heterogeneous model of a fixed packed-bed reactor is derived, which constitutes one set of equations for the reactor and one set of equations for the catalyst pellet. In this model we have taken the same assumptions

for the pseudo-homogeneous reactor model along with one more assumption: all catalyst pellets are of the same size and the voids between are evenly distributed.[44,45]

In the present study, a parallel pore model is adopted for the pellet to simplify the complex structure of voids where the fluid may flow; that is, we employ in some respect a general mathematical model of a spherical pellet where reactions take place on active sites within a uniform body. Thus, the mathematical model used in this work assumes a mean pore diameter and the ratio between the porosity and tortuosity is used to characterise a fixed structure of the pellet. Possible structural changes are not considered.

Bulk gas equations

A cross-sectional average of Equation (2) reduces the model to a one-dimensional species mass balance equation:

$$\frac{\partial(\epsilon_b \rho_g w_j)}{\partial t} + \frac{\partial}{\partial z}(\rho_g w_j u_z) + \frac{\partial(\epsilon_b J_j)}{\partial z} = a_v k_j \rho_g (w^s_{p,j} - w_j) \tag{21}$$

It is noted that Equation (21) is not derived explicitly from Equation (2). Diffusive flux J_j has been calulated by Equation (5). The mass transfer coefficient values are computed from correlation with dimensionless numbers:[47]

$$Sh = 2 + 1.1 Sc^{1/3} Re_p^{0.6} \qquad 3 < Re_p < 10\,000 \tag{22}$$

The continuity can be obtained by adding up the species balances (21) for all the species with constraints, $\sum_{j=1}^{N} w_j = 1$ and $\sum_{j=1}^{N} J_j = 0$, which results in:

$$\epsilon_b \frac{\partial \rho_g}{\partial t} + \frac{\partial}{\partial z}(u_z \rho_g) = \sum_{j=1}^{N} a_v k_j \rho_g (w^s_{p,j} - w_j) \tag{23}$$

A one-dimensional energy equation is formulated in terms of temperature:

$$\left((1-\epsilon_b) Cp'_p \rho_p + \epsilon_b \rho_g Cp_g\right) \frac{\partial T}{\partial t} + \rho_g Cp_g u_z \frac{\partial T}{\partial z} = -\frac{\partial}{\partial z}(Q_z) + a_v h (T^s_p - T) + \frac{4U}{d_t}(T_w - T) \tag{24}$$

The second term on the right hand side of the above equation is the heat removed at the surface of the catalyst particles. The heat flux Q_z and the Ergun equation have been described in Equations (16) and (11). The heat-transfer coefficient between the gas phase and the particles is calculated using analogy between heat and mass transfer, replacing Sh and Sc with Nu and Pr numbers, respectively.

$$Nu = 2 + 1.1 Pr^{1/3} Re_p^{0.6} \tag{25}$$

The ideal gas law has been used to calculate mixture density in the gas phase.

Pellet equations

For a symmetric sphere, Equation (2) reduces to a one-dimensional model, hence the transport equation for porous sphere may be given as:

$$\epsilon \frac{\partial}{\partial t}(\rho_g w^s_{p,j}) + \frac{1}{r^2}\frac{\partial}{\partial r}(r^2 u_r \rho_g w^s_{p,j}) = -\frac{1}{r^2}\frac{\partial}{\partial r}(r^2 \mathbf{J}_{j,r}) + S_{w_j} \tag{26}$$

where $\mathbf{J}_j$ is the mass based diffusion flux defined later in Equations (34), (38), and (39). The second term on the left hand side of the above equation is the viscous term which is usually neglected. Hence, simulation with and without the viscous term is needed in order to validate whether this term affects the overall reactor performance or not. The source density of species mass balance is:

$$S_{wj} = (1-\epsilon)\rho_{cat} M_j \sum_{k=1}^{3} \mathbf{R}_k \nu_{jk} \tag{27}$$

The continuity can be obtained by adding up the species balances (27) for all the species with constraints, $\sum_{j=1}^{N} w_j = 1$ and $\sum_{j=1}^{N} J_j = 0$, which results in:

$$\epsilon \frac{\partial \rho_g}{\partial t} + \frac{1}{r^2}\frac{\partial}{\partial r}(r^2 u_r \rho_g) = \sum_{j=1}^{N} S_{w_j} \tag{28}$$

A consistent one-dimensional heat equation in terms of temperature yields for the solid phase:

$$\left((1-\epsilon) C'_{p_p} \rho_p + \epsilon \rho_g \sum_{j=1}^{N} w_j Cp_j\right) \frac{\partial T}{\partial t} + \rho_g \sum_{j=1}^{N} w_j Cp_j u_r \frac{\partial T}{\partial r} = -\frac{1}{r^2}\frac{\partial}{\partial r}(r^2 Q_r) + S'_T \tag{29}$$

Source density of temperature equation:

$$S'_T = (1-\epsilon)\rho_{cat} \sum_{k=1}^{3} (-\Delta H_{r_k}) \mathbf{R}_k \tag{30}$$

The heat flux is defined by Fourier's law:

$$Q_r = -\lambda \frac{\partial T}{\partial r} \tag{31}$$

where the λ values for the solid and gas conductivity have been estimated from Yaws.[48] The viscous gas velocity in the catalyst pores is driven by a pressure gradient that is caused by temperature evolution created by chemical reactions and the potential non-uniform spatial species composition.

Darcy's law represents the relation between viscous gas velocity and pressure gradient:[18,14]

$$u_r = -\frac{\beta_0}{\mu}\nabla p \tag{32}$$

In the parallel-pore model, pores are assumed to be cylindrical, hence the permeability can be computed from the Poiseuille flow relationship:[18]

$$\beta_0 = \frac{\epsilon}{\tau}\frac{d_0^2}{32} \tag{33}$$

where the porosity-tortuosity factor ϵ/τ is introduced to characterize the pellet structure.

The ideal gas law has been used to calculate mixture density in the solid phase. Several diffusion flux models have been used to close the species mass balance. In our model, we have used 4 different diffusion flux closures:

Table 1. Initial and boundary conditions for the pseudo-homogeneous model and bulk gas phase equations of conventional and simplified heterogeneous reactor models

Initial conditions

$$\left.\begin{array}{c} w_j = w_{j,\,in} \\ T = T_{in} \\ \rho_g = \rho_{g,\,in} \end{array}\right\} \quad \text{for} \quad t = 0,\ \forall\, z \tag{52}$$

Boundary conditions

Boundary condition for the velocity derivative in the continuity equation:

$$u_z = u_{in} \qquad \text{for} \qquad z = 0 \tag{53}$$

Boundary conditions for the differentiated variable w_j in the species mass balance equation:

$$(w_j \rho_g u_z)(0^+, t) = (\rho_{g,\,in} u_{in} w_{j,\,in})(0, t) - J_j(0^+, t) \quad \text{for} \quad z = 0 \tag{54}$$

For the diffusion flux equation:

$$J_j = 0 \quad \text{for} \quad z = L \tag{55}$$

Boundary conditions for the differentiated variable T in the energy equation:

$$(Q_z \lambda)(0^+, t) + (Cp_g u_z \rho_g T)(0^+, t) = (Cp_g u_{in} \rho_{g,\,in} T_{in})(0, t) \quad \text{for} \quad z = 0 \tag{56}$$

For the heat flux equation:

$$Q_z = 0 \quad \text{for} \quad z = L \tag{57}$$

Boundary condition for the pressure derivative:

$$P = P_{in} \quad \text{for} \quad z = 0 \tag{58}$$

1. The Mass-based Wilke model for bulk diffusion:[14]

$$\mathbf{J}_j = -\rho_g D^e_{jm} \nabla w_j \tag{34}$$

where the mass-based Wilke effective diffusion coefficient is represented by:

$$D^e_{jm} = \left(M_w \sum_{\substack{i=1 \\ i \neq j}}^{n} \frac{w_i}{M_{w_i} D^e_{ji}} \right)^{-1} \tag{35}$$

It is noted that the Wilke equation does not generally satisfy the constraints, $\sum_{j=1}^{N} w_j = 1$ and $\sum_{j=1}^{N} J_j = 0$.[49,14]

2. If Knudsen diffusion is important, the Wilke model is modified by applying the Bosanquet approach:[50,14]

$$\mathbf{J}_j = -\rho_g D^e_{j,eff} \nabla w_j \tag{36}$$

where:[50,14]

$$\frac{1}{D^e_{j,eff}} = \frac{1}{D^e_{jm}} + \frac{1}{D^e_{jk}} \tag{37}$$

Table 2. Boundary conditions for particle equations of the conventional heterogeneous reactor model

Boundary conditions

Boundary condition for the species mass balance equation:

$$\mathbf{J}_{j,r} = 0 \quad \text{for} \quad r = 0 \quad \text{(due to symmetry)} \tag{59}$$

For the differentiated variable x_j in the diffusion flux equation:

$$\mathbf{J}_{j,r} + u_r \rho_g w_j = -k_j (\rho^b_{j,g} - w_j \rho_g) \quad \text{for} \quad r = r_p \tag{60}$$

Boundary condition for the temperature equation:

$$Q_r = 0 \quad \text{for} \quad r = 0 \quad \text{(due to symmetry)} \tag{61}$$

For the differentiated variable T in the heat flux equation:

$$\rho_g Cp_g u_r T + Q_r = -h(T^b - T) \quad \text{for} \quad r = r_p \tag{62}$$

For the differentiated variable ρ_g in the continuity equation:

$$\rho_g = \rho^b_g \quad \text{for} \quad r = r_p \tag{63}$$

For Darcy's law:

$$\frac{\partial p}{\partial r} = 0 \quad \text{for} \quad r = 0 \tag{64}$$

3. The Explicit Mass-based Maxwell-Stefan model:[14]

$$\mathbf{J}_j = \frac{\frac{M_w}{\rho_g} \sum_{\substack{i=1 \\ i \neq j}}^{N} \frac{w_j J_i}{M_{w_i} D^e_{ji}} - w_j \nabla ln(M_w) - \nabla w_j}{\frac{M_w}{\rho_g} \sum_{\substack{i=1 \\ i \neq j}}^{N} \frac{w_i}{M_{w_i} D^e_{ji}}} \tag{38}$$

The multicomponent Maxwell-Stefan model can give more accurate results for multicomponent mixtures in comparison to the approximated results obtained by use of the

Table 3. Reactor specification for the SMR process[12,61]

Mass fractions		
CH_4	0.1911	–
CO	0.0001	–
CO_2	0.0200	–
H_2	0.0029	–
H_2O	0.7218	–
N_2	0.0641	–
Inlet pressure	$29 \cdot 10^5$	Pa
Tube inlet temperature	793	K
Tube outlet temperature	1048	K
Physical Parameters		
Density of catalyst	2300	kg cat/m^3
Pellet void fraction	0.528	–
Pellet diameter	0.0173	m
Tortuosity	3.5	–
Mean pore diameter[7]	100	nm
Heat capacity of solids	850	J/kgK
Tube inner diameter	0.1016	m
Tube outer diameter	0.1322	m
Length of tube	7	m
Inlet superficial velocity	1.89	m/sec

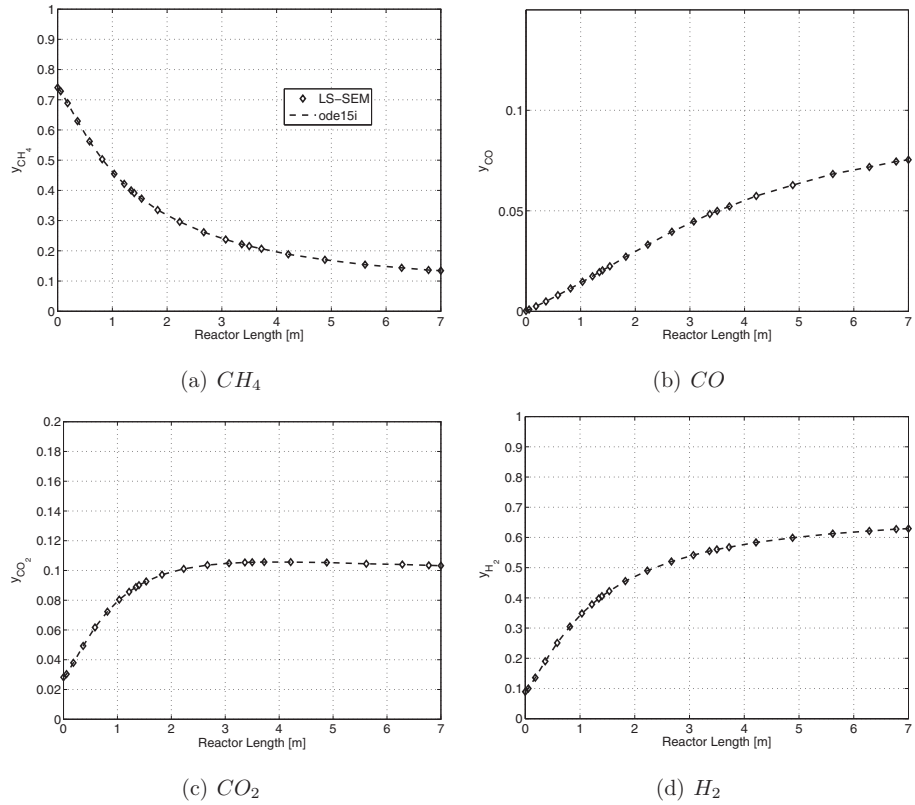

(a) CH_4 (b) CO

(c) CO_2 (d) H_2

Figure 1. Steady-state axial distribution of component concentration in the pseudo-homogeneous fixed bed reactor model for the SMR process using LS-SEM and ode15i MATLAB.

extended Fick diffusion flux model originally designed for binary mixtures.[18]

4. The Explicit Mass-based dusty gas model:[14]

$$J_j = \frac{M_w^2 \sum_{\substack{i=1 \\ i \neq j}}^{n} \frac{w_j J_i}{M_{w_i} D_{ji}^e} - \frac{\mathbf{v}\,\rho_j M_w}{D_{jk}^k} - \rho(w_j \nabla M_w + M_w \nabla w_j)}{M_w^2 \sum_{\substack{i=1 \\ i \neq j}}^{n} \frac{w_i}{M_{w_i} D_{ji}^e} + \frac{M_w}{D_{jk}^e}} \quad (39)$$

where D_{jK}^e can be expressed as:[51]

$$D_{jk}^e = 97.0\, r (T/M_j)^{0.5} \quad (40)$$

The dusty gas approach attempts to provide a more realistic description of the diffusion mechanism in the combined bulk and Knudsen regime based on the Maxwell-Stefan approach.

The porous pellets consist of interconnected nonuniform pores into which the fluid may flow. Hence, in this study the effective diffusion coefficient is related to the molecular diffusion coefficient by $D^e = D(\epsilon/\tau)$ according to the parallel pore model. Data on diffusion coefficients at high temperatures and pressures are rare. Therefore, the binary diffusion coefficients were estimated by the Fuller, Schettler, and Giddings (FSG) equation:[15]

$$D_{i,j} = \frac{10^{-4} T^{1.75} (M_i^{-1})^{0.5}}{P_{atm} (\sum \upsilon_i^{1/3} + \sum \upsilon_j^{1/3})^2} \quad (41)$$

Simplified Heterogeneous Fixed Bed Reactor Model

Bulk gas equations[16,17]

Bulk gas phase equations of the simplified heterogeneous model are the same as the conventional heterogeneous model.

Pellet equations[16,17]

The transport equation for porous spheres may be given as:

$$\epsilon_p \frac{\partial}{\partial t}(\rho_g w_{p,j}^s) = a_v k_j \rho_g (w_j - w_{p,j}^s) + (1-\epsilon_p)\rho_{cat} \sum_{k=1}^{3} \eta_k \mathbf{R}_k \nu_{jk} \quad (42)$$

The temperature equation is given as:

$$\left((1-\epsilon) C_{p_p}' \rho_p + \epsilon \rho_g \sum_{j=1}^{n} w_j Cp_j\right) \frac{\partial T_p^s}{\partial t} + \rho_g \sum_{j=1}^{n} w_j Cp_j u_r \frac{\partial T}{\partial r} = a_v h (T - T_p^s) + S^T \quad (43)$$

The source term (S^T) in the above temperature equation is given as:

$$S^T = (1-\epsilon_b)\rho_{cat} \sum_{k=1}^{3} (-\Delta H_{r_k}) \eta_k \mathbf{R}_k \quad (44)$$

Initial and Boundary Conditions for Different Reactor Models

Table 1 gives the initial and boundary conditions of the pseudo-homogeneous reactor model, and bulk gas phase equations of the conventional and simplified heterogeneous reactor models. Table 2 shows the boundary conditions of the particle equations

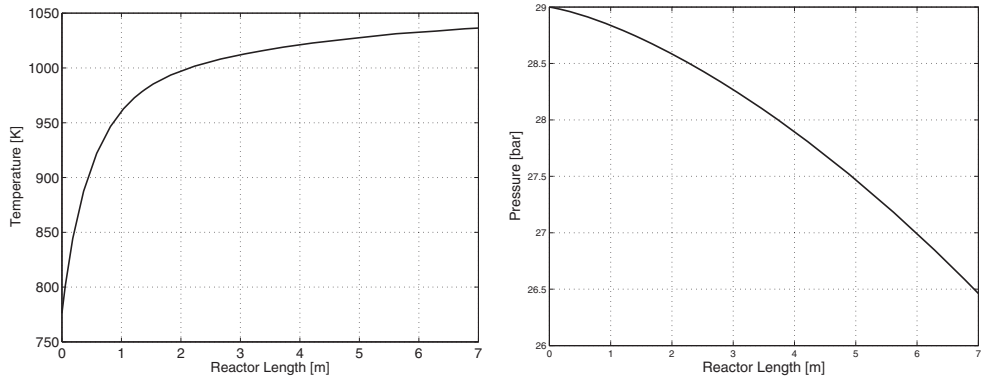

(a) *Temperature* (b) *Pressure*

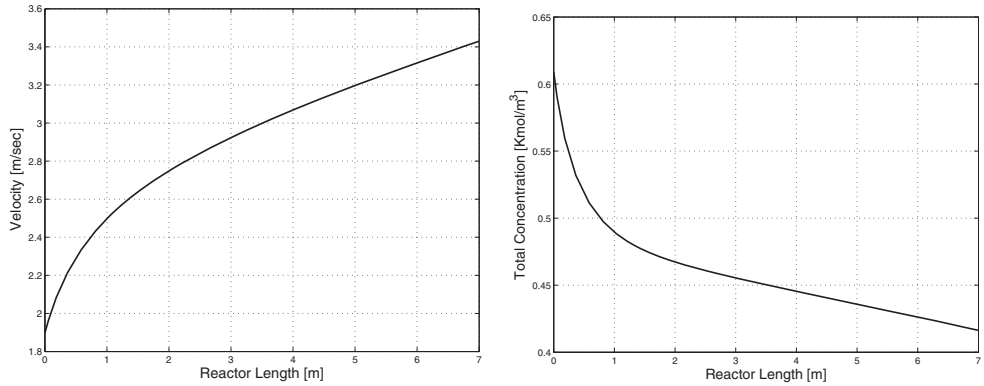

(c) *Velocity* (d) *Total Concentration*

Figure 2. Results obtained in the simulation of the pseudo-homogeneous fixed bed reactor model for the SMR process.

of the heterogeneous model. It is noted that initial conditions of the particle equations of the conventional and simplified heterogeneous models vary at each time step of the gas phase equations.

Chemical Model

Steam methane reforming on nickel-based catalysts is the main process for industrial production of hydrogen or synthesis gas. Numerous studies have been reported on the kinetics of these reactions.[52–54] Xu and Froment[5,6] developed a kinetic rate model for the steam methane reforming process on a Langmuir-Hinshelwood mechanism formed of 13 steps, 3 of which are rate determining and the rest are at equilibrium. They considered the main steam reforming reactions in addition to the water-gas shift reaction, and their network has been represented by Reactions (I–III). Their rate equations were used in our simulations:

$$\mathbf{R}_1 = \frac{k_1}{p_{H_2}^{2.5}}\left[\frac{p_{CH_4}p_{H_2O} - p_{H_2}^3 p_{CO}/K_1}{DEN^2}\right] \tag{45}$$

$$\mathbf{R}_2 = \frac{k_2}{p_{H_2}}\left[\frac{p_{CO}p_{H_2O} - p_{H_2}p_{CO_2}/K_2}{DEN^2}\right] \tag{46}$$

$$\mathbf{R}_3 = \frac{k_3}{p_{H_2}^{3.5}}\left[\frac{p_{CH_4}p_{H_2O}^2 - p_{H_2}^4 p_{CO_2}/K_3}{DEN^2}\right] \tag{47}$$

where

$$DEN = 1 + K_{CO}p_{CO} + K_{H_2}p_{H_2} + K_{CH_4}p_{CH_4} + K_{H_2O}p_{H_2O}/p_{H_2} \tag{48}$$

$\mathbf{R}_1$, $\mathbf{R}_2$, $\mathbf{R}_3$ correspond to Reactions (I), (II) and (III), respectively. All rate and adsorption constants are given by Xu and Froment.[5,6]

MODEL SOLUTION

In engineering practice, the conservation equations are normally solved by the finite difference method (FDM)[55–58] and the finite volume method (FVM).[59] Other methods may be more appropriate for equations with particular mathematical characterstics or when more accurate, robust, stable, and efficient solutions are required. The alternative spectral methods can be classified as sub-groups of the general approximation technique for solving differential equations, named the method of weighted residuals (MWR). It is popular because of the interactive nature of the first step; that is, the user provides a first guess at the solution and this is then forced to satisfy the governing equations along with the conditions imposed at the boundaries.[60] The left-over terms, called residuals, arise because the chosen form of the solution does not exactly satisfy either the equation or the boundary conditions. However, these residual terms are minimized providing the basis for parameter or function selection. Of course, the optimum solution depends on the intelligent selection of a proposed solution. There are five widely-used variations of the method of weighted residuals for engineering applications.

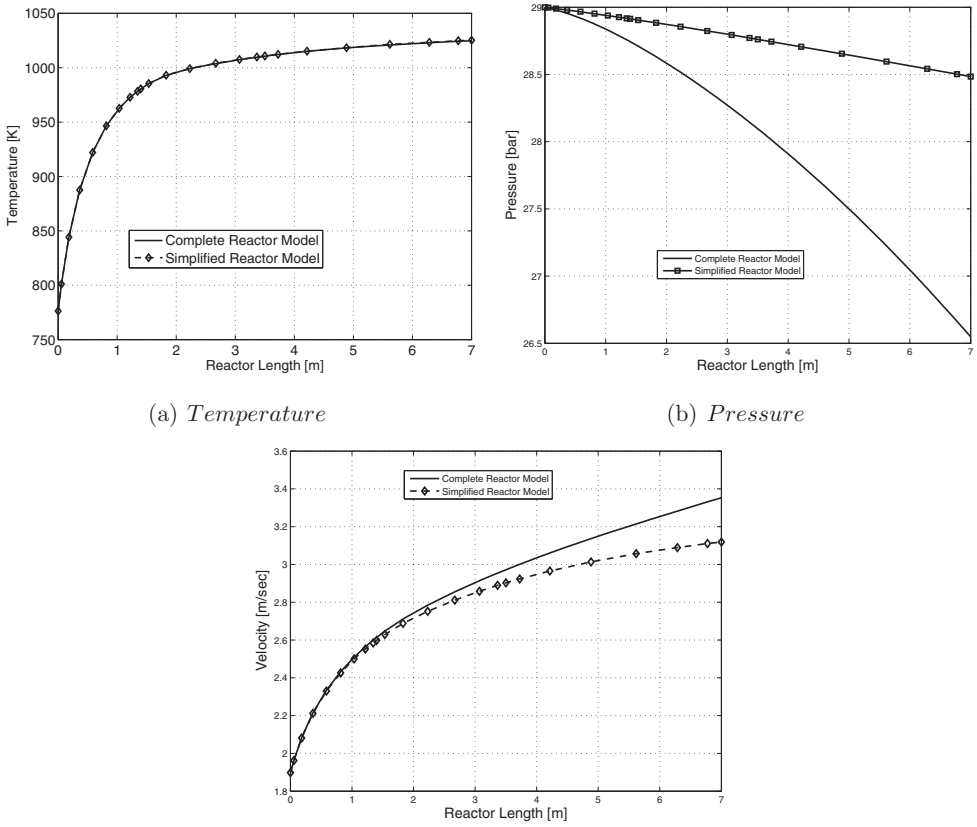

(a) *Temperature* (b) *Pressure*

(c) *Velocity*

Figure 3. Comparison between the complete and simplified pseudo-homogeneous reactor models for the SMR process.

They are distinguished by the choice of the test functions, used in the minimization of the residuals. These five methods are: the collocation, subdomain, least-squares, moment, and Galerkin methods. These methods can also be applied to subdomains. The subdomain methods are generally devided into two categories: the spectral element[62,63] and finite element[64,65] methods. In the spectral element methods, the solution on each subdomain is approximated by high order polynomial expansion. In the finite element methods, on the other hand, the solution of each element is normally approximated by a first order (low order) polynomial expansion.[66] It is noted that for a given accuracy the high order spectral method requires only a few collocation points, whereas the low order methods, such as the FVM, require a large number of grid points. The time dependent governing equations for the different fixed bed reactor models are solved using the least-squares spectral element methods (LS-SEM).[7,10,61] The basic idea in the LSM is to minimize the integral of the square of the residual over the computational domain.

For the case of pellet modelling for conventional heterogeneous reactor models, symmetry is assumed in the sphere which results in one independent spatial variable in the radial dimension which is discretized with the method of weighted residuals concepts, whereas for the case of gas phase equations of reactor models, it has been discretized across the axial direction of the reactor. The Gauss-Labatto-Legendre (GLL) collocation points are used. This well-known theta-method has been used to discretize the transient terms in the governing equations. In our simulations, we have used a backward differencing scheme, i.e., $\theta = 0$. The computational domain of the reactor has been divided into 3 elements with 23 collocation points, whereas the computational domain of the pellet has been divided into 3 elements with 14 collocation points.

In order to assess the convergence of the model, we define two convergence criteria:

$$Residual = \sqrt{\langle \mathcal{L}' f_N - g, \mathcal{L}' f_N - g \rangle} \leq e^{-5} \tag{49}$$

$$\varepsilon_{iteration} = \sqrt{{f_N}^{it} - {f_N}^{it-1}, {f_N}^{it} - {f_N}^{it-1}} \leq e^{-10} \tag{50}$$

The residual denotes a measure for the overall error obtained for the system of equations discretized by the least squares method. The iteration overall error denotes a measure of the difference in variable values between the second-last and last preceding iterations, for a preliminary $\mathcal{L}'$ representing a linearized integro-differential operator using the Picard iteration technique. The iteration procedure proceeds to update the $\mathcal{L}'$ estimates until both error measures are less than the specified upper limits.

In the heterogeneous model, the particle equations are solved until convergence is reached with specified bulk conditions at a specified time step at each collocation point of the reactor. Then, the gas phase equations are solved until convergence is reached for the specified time step. The governing equation in the LS-SEM solution process, which is a system of nondimensionalized model equations, has been used.

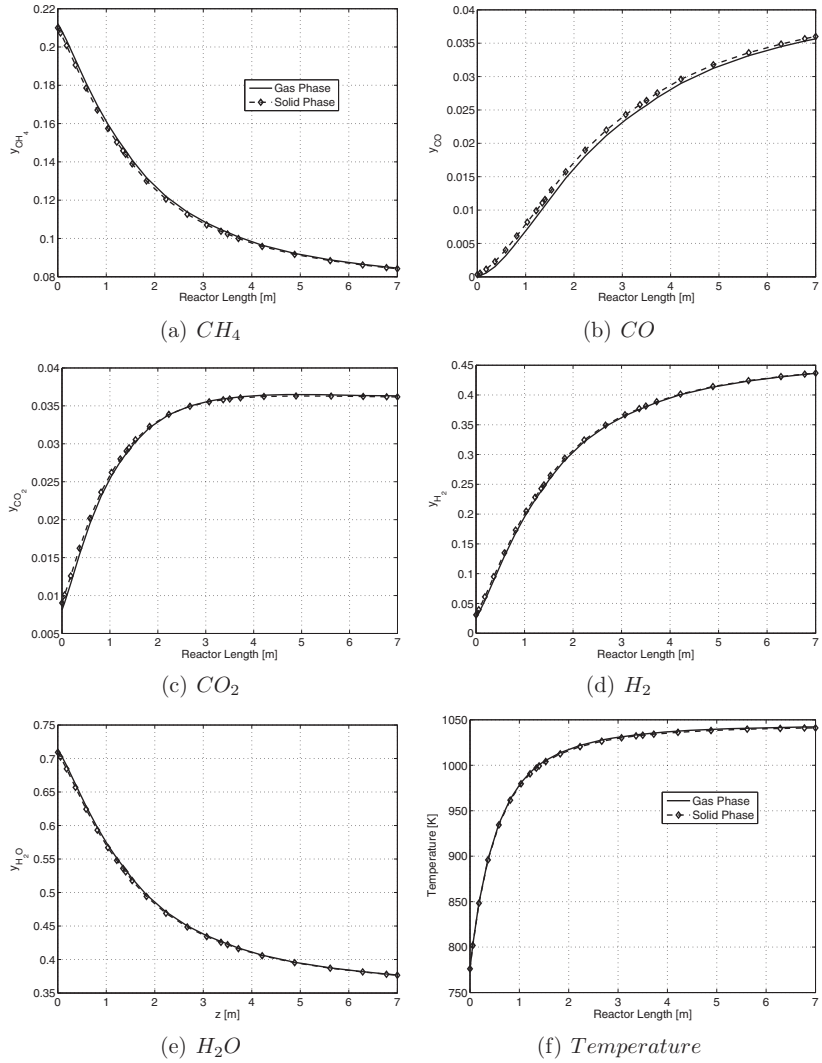

(a) CH_4 (b) CO

(c) CO_2 (d) H_2

(e) H_2O (f) $Temperature$

Figure 4. Comparison of mole fraction profiles of different components and temperature profiles along the reactor axis between fluid and solid phases of the conventional heterogeneous reactor model under steady-state conditions.

RESULTS AND DISCUSSION

The mass-based dynamic pseudo-homogeneous, conventional heterogeneous, and simplified heterogeneous reactor models applied to the steam methane reforming process describe the evolution of species mass fraction, pressure, mixture density, temperature, mass diffusion flux, heat flux, and convection flux. The reactor model equations have been solved by the least-squares spectral element method. Effects of solving the momentum equation instead of Ergun's equation on the reactor performance have been studied. This section also presents the need for the heterogeneous model for the steam methane reforming process instead of the pseudo-homogeneous model. Furthermore, a numerical comparison of pseudo-homogeneous, conventional, and simplified heterogeneous reactor models has been made to study the impact on axial profiles along the reactor. The impacts of the mass diffusion fluxes on the reactor performance have been studied. A tube reactor with dimensions and input conditions given in Table 3 is simulated.

General Physics of the SMR process

A measure used for the performance of the reactor is the dry mole fraction of different components, which is the mole fraction of different components of the gas after the steam content has been removed. The dry mole fractions are calculated as:

$$x_i^d = \frac{x_i}{1 - x_{H_2O}} \tag{51}$$

Figure 1 is plotted using Equation (51). We performed a preliminary validation of the solver LS-SEM to confirm the results obtained for the pseudo-homogeneous fixed bed reactor model. For this, we compared the results obtained with an established solver against those obtained using the solver based on the LS-SEM. The established solver is the ode15i present in the MATLAB software package. Figure 1 presents the results of the mole fractions profiles of the SMR process using both the MATLAB and LS-SEM solvers. Both solvers showed good accordance. It can be seen from Figure 1 that the component concentration increases for the products, i.e., carbon dioxide, carbon monoxide, and hydrogen, and decreases for the reactant methane across the reactor axis. In the synthesis gas process CO is produced from CH_4 and H_2O. The reversed water gas shift reaction consumes CO in the reactor axis from 0 to 2 m. The mole fraction of CO_2 increases moving away from the reactor entrance and reaches a maximum at a distance of 2 m from the inlet. At reactor length equal to

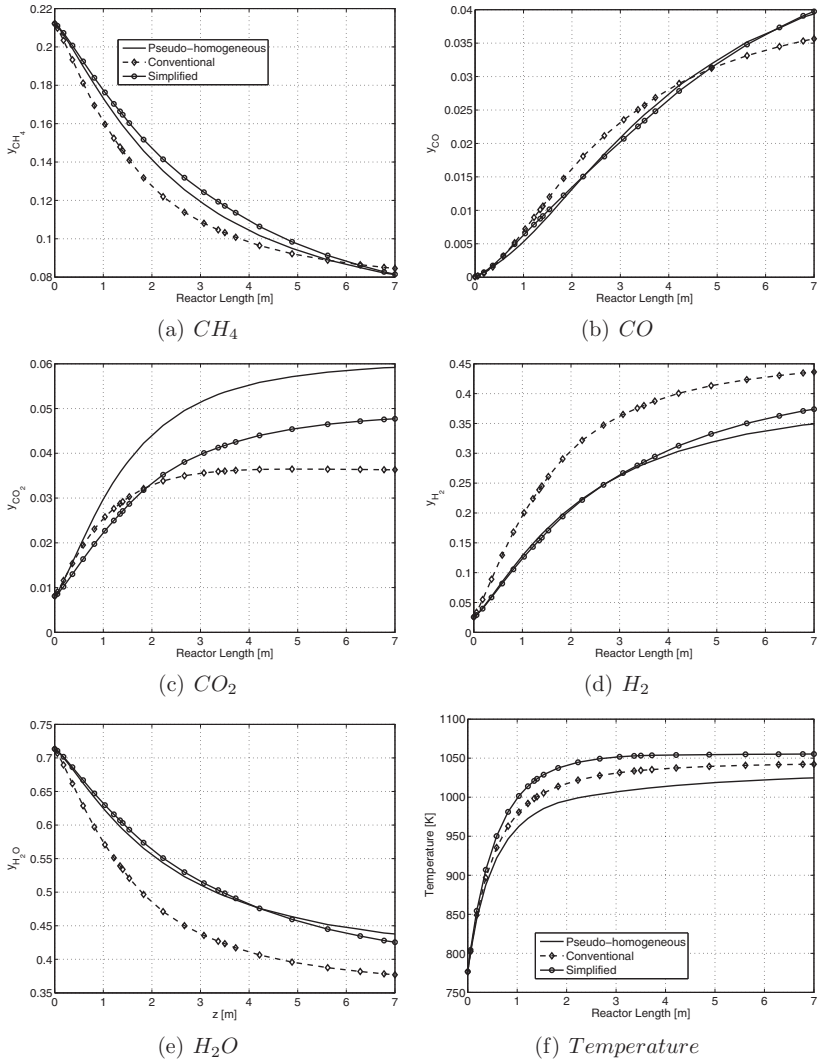

(a) CH_4 (b) CO

(c) CO_2 (d) H_2

(e) H_2O (f) $Temperature$

Figure 5. Comparison of gas phase mole fraction profiles of different components and temperature profiles along the reactor axis between the pseudo-homogeneous, conventional heterogeneous, and simplified heterogeneous reactor models under steady-state conditions.

2 m, the reaction is reversed, and a maximum occurs in the CO_2 profile. Then, there is a slight decrease to the point where equilibrium is achieved. The gradient of the CO-profile is not very steep at the reactor entrance. However, it gets steeper in the interval of 0.25–1 m. Further away from the entrance, the profile flattens until equilibrium is achieved about 6 m into the reactor.

At the entrance of the reactor, there is a slight decrease in temperature, and then an increase along the rest of the length of the reactor as shown in Figure 2a. The concentration of the reactants is high at the inlet, so the reaction rate predominates in the beginning, which leads to high consumption of the heat provided by the reformer furnace because the overall reaction taking place is endothermic. Since the concentration of the reactants starts to decrease, meaning that the reaction rate declines, the temperature tends to increase. The temperature profile at reactor length approximately equal to 6 m is nearly flat, which can be explained due to the reaction rate becoming such that the heat consumed by the reaction is comparable to the heat supply from the heating. According to Ergun's equations, total partial pressure directly depends on the velocity. Figure 2c shows that the velocity increases along the reactor axis. So, the pressure of the gas as shown in Figure 2b drops along the tube. As the total concentration has been calculated from the ideal gas law, the change of the total concentration depends on the total pressure and temperature behaviour through the reactor length. Convective flux dominates over the diffusive flux along the reactor axis for the fixed bed reactor. This supports the commonly adopted assumption of neglecting the diffusive flux in the reactor model. This conclusion relies on the magnitude of the gas velocity in the reactor; for very low gas flow rates the dispersion term might be more important.

Effects of Solving the Momentum Equation

The pseudo-homogeneous reactor model with the pressure-velocity coupling equation, i.e., Equation (10), is referred as the complete reactor model, whereas the reactor model with Ergun's equation is only named the simplified reactor model in this manuscript.

Comparisons of the pressure, velocity, temperature, and mole fraction profiles of different components that were obtained in the reactor are shown in Figures 3–4, respectively. As seen in Figures 3b–c, the pressure and velocity in the reactor are clearly different in both cases. However, the difference is quite small. Hence, these phenomena do not affect the solution of all other transport equations.

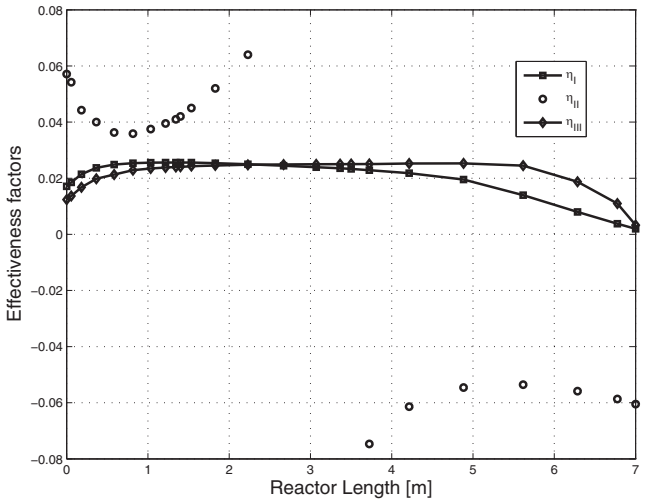

Figure 6. Effectiveness factors in the SMR process under steady-state operation using the conventional heterogeneous reactor model.

The Ergun equation is not on a transient form; hence, the pressure will be set up instantaneously as a function of velocity. Because the pressure, in reality, has a fast but dynamic nature, the simplifications in the Ergun equation can lead to numerical problems. With certain combinations of initial and operating conditions, nonphysical solutions such as a reversal of the flow in the reactor may occur: these are solutions that are not observed when using the more rigorous model. Therefore, the rigorous model is chosen to be able to handle different types of operating conditions, although it is computationally more expensive. However, for the SMR process, the simplified reactor model should be replaced with the computationally expensive complete reactor model for future modelling and model-based activities.

Heterogeneous Reactor Model

The conventional heterogeneous model was analyzed at steady-state conditions to see whether the difference between the two phases is considerable or not. It was observed that there is a considerable difference between the behaviour of the variables in the solid and fluid phases. That is, the profiles of mole fractions of components along the reactor did not have completely the same patterns in the solid and fluid phases under steady-state conditions. This is illustrated in Figure 4. This suggests that the heterogeneous reactor model is needed for the SMR process. Therefore, a complete comparison should be done for the case of homogeneous and heterogeneous reactor models to find out the exact amount of deviation between the two. In this conventional heterogeneous model, the Maxwell-Stefan closure is used for the intra-particle mass diffusion flux.

The maximum deviation between the fluid and solid phases is less than 3 %. The difference of fluid and solid phases is much higher near the entrance of the reactor. This difference is related to the external mass transfer regime. Near to the inlet of the reactor, the reactants diffuse on the surface of the catalyst pellets and immediately convert out from the catalyst pellets, causing differences between the solid and fluid phases. Moreover, as the axial length of the reactor increases, the two phases behave more similarly to each other. The similarity between the solid and fluid concentrations indicates the controlling phenomenon is the kinetic reaction. It should be noted that as the axial length increases, the two phases behave much more similarly to each other. For the limiting case of the reactor outlet, as it is observed, the two phases become identical, which is a good result for estimation and control of outlet stream which is a practical issue. It is undoubtedly true that for industrial reactors, the higher linear velocity of the reactant stream causes such similar behaviours in the gas and solid phases.

Comparison of Pseudo-Homogeneous, Conventional Heterogeneous, and Simplified Heterogeneous Reactor Models for the SMR Process

For the case of pseudo-homogeneous and simplified heterogeneous reactor models, effectiveness factors are used for the reforming and water-gas shift reactions to account for internal diffusion resistance. The effectiveness factors are found from simulations of one catalyst pellet with typical bulk gas phase compositions as boundary conditions, and were found to be 0.01, 0.07, and 0.008 for the reactions in Reactions (I–III), respectively.[67] These values are used in the simulation of pseudo-homogeneous and simplified heterogeneous reactor models.

Figure 5 shows the comparison of the pseudo-homogeneous, conventional, and simplified heterogeneous reactor models for the SMR process. Figures 5a–e show the mole fraction profiles of different components of the gas phase along the reactor axis that were obtained from the simulation of different reactor models under steady-state conditions. It has been found that the maximum deviation between the pseudo-homogeneous and conventional heterogeneous models is less than 38 %, whereas the deviation between the conventional and simplified heterogeneous reactor models is less than 21 %. Furthermore, the percentage of deviation increases with the length of the reactor. This signifies that the assumptions of a constant effectiveness factor along the reactor axis, and negligence of heat and mass exchange between the solid and gas phases, are not correct. The smaller deviation between the simplified and conventional heterogeneous reactor models is due to the simplified heterogeneous reactor model containing the mass and heat exchange between the solid and gas phases. Hence, Figure 5f shows that the deviation between the temperature profiles of the gas phase for the simplified and conventional heterogeneous reactor models is smaller than the pseudo-homogeneous and conventional heterogeneous reactor models.

Figure 6 shows the effectiveness factor values of the reforming and water gas shift reactions along the reactor axis which have been calculated from the conventional heterogeneous reactor model. The effectiveness factors of Reactions (I) and (II) both decrease through the reactor. When the reaction is near equilibrium, the reaction rate is more sensitive with respect to changes in concentration. This is because the rate of the reverse reaction increases with a similar value as the reduction in rate of the forward reaction. The values of the effectiveness factors η_1 and η_3 obtained in this study are close to the values found in the literature.[6,68,8] Hence, it is seen that the SMR process is a diffusion limited process with very low effectiveness factors (less than 0.03). The η_2 value has an asymptote at z = 2.2 m. Following the analysis of Xu and Froment,[6] Pantoleontos et al.[8] and Pedernera et al.[69] found that this discontinuity is due to the change of the water gas shift reaction's direction. As the effectiveness factor values of the SMR process are in close agreement with the literature values, it is assumed that the conventional heterogeneous model is the best choice for the SMR process. However, it is noted that the intra-particle mass diffusion flux of the conventional heterogeneous model can be described by Maxwell-Stefan, Wilke, dusty gas, and Wilke-Bosanquet closures. Hence, the effects of

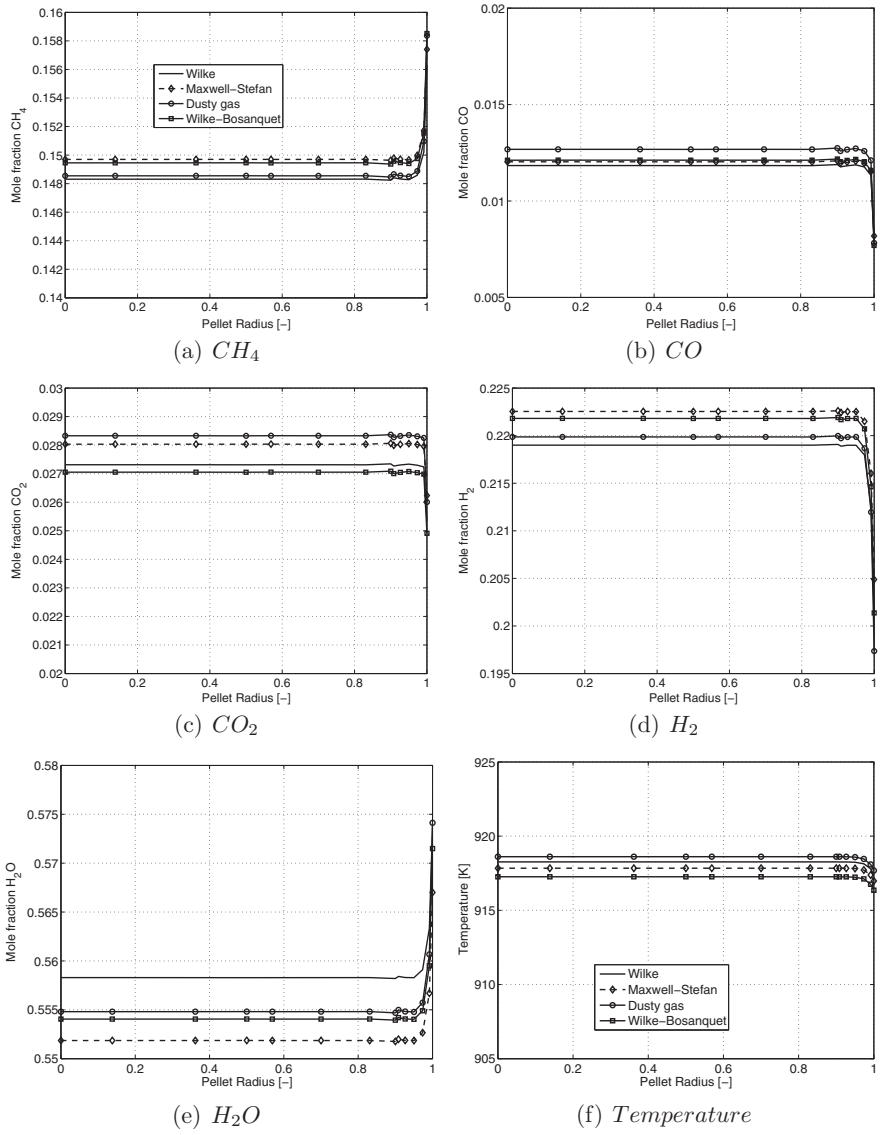

Figure 7. Mole fraction profiles of different components of the SMR process. Effects of several diffusion models on pellet level at a distance of 1 m from the entrance of the reactor; Wilke, Maxwell-Stefan, dusty gas, and Wilke-Bosanquet models.

the Maxwell-Stefan, Wilke, dusty gas, and Wilke-Bosanquet mass diffusion fluxes on the reactor performance should be studied.

Intra-Particle Mass Diffusion Models

The conventional heterogeneous model, where the intra-particle mass diffusion in the voids of pellets is described by the Wilke model, was studied by many researchers for the SMR process. All of the researchers[25–28] coupled the pellet model with the fixed-bed reactor balance equations along with some basic assumptions adopted for the catalyst pellet; for example, they neglected pressure changes inside the pellet, effects of Knudsen diffusion and viscous flow were disregarded, and the pellets were modelled as isotropic with respect to porosity, tortuosity, pore size distribution, and conductivity. However, there is a basic argument that the differences between the various diffusion flux models, i.e., Wilke, Maxwell-Stefan, dusty gas, and Wilke-Bosanquet, cannot always be neglected a priori if a detailed calculation of the concentration profiles in the pellet is desired. None of the research studied the effect of various flux models on the reactor performance for the SMR process. Thus, in the present study we have studied the SMR process by adopting a conventional heterogeneous reactor model where intra-particle mass diffusion flux is described by several closures (Wilke, Maxwell-Stefan, dusty gas, and Wilke-Bosanquet) elucidating the effects of viscous flow and variable pressure within the pellet.

Figures 7–8 hold the mole fraction profiles for the SMR process on the pellet level and the reactor level, respectively. It is found that the results of the dusty gas and Wilke-Bosanquet models are different than the Maxwell-Stefan model. The reason for this is that both the dusty gas and Wilke-Bosanquet models consider the Knudsen diffusion. It is noted that the Wilke equation does not satisfy the constraints. From Figure 8, it is evident that the mole fractions of CO and H_2O for the Wilke model at the reactor exit are smaller than other diffusion models. Due to the water gas shift reaction the mole fractions of H_2 and CO_2 should be higher. However, it is found from Figure 8c that the mole fraction of CO_2 for the Wilke model is lower than for other diffusion models. This inconsistency is due to the Wilke model, which does not satisfy the constraints. To deepen the analysis further, Figure 8 shows the mole fraction profiles of the different components for the SMR

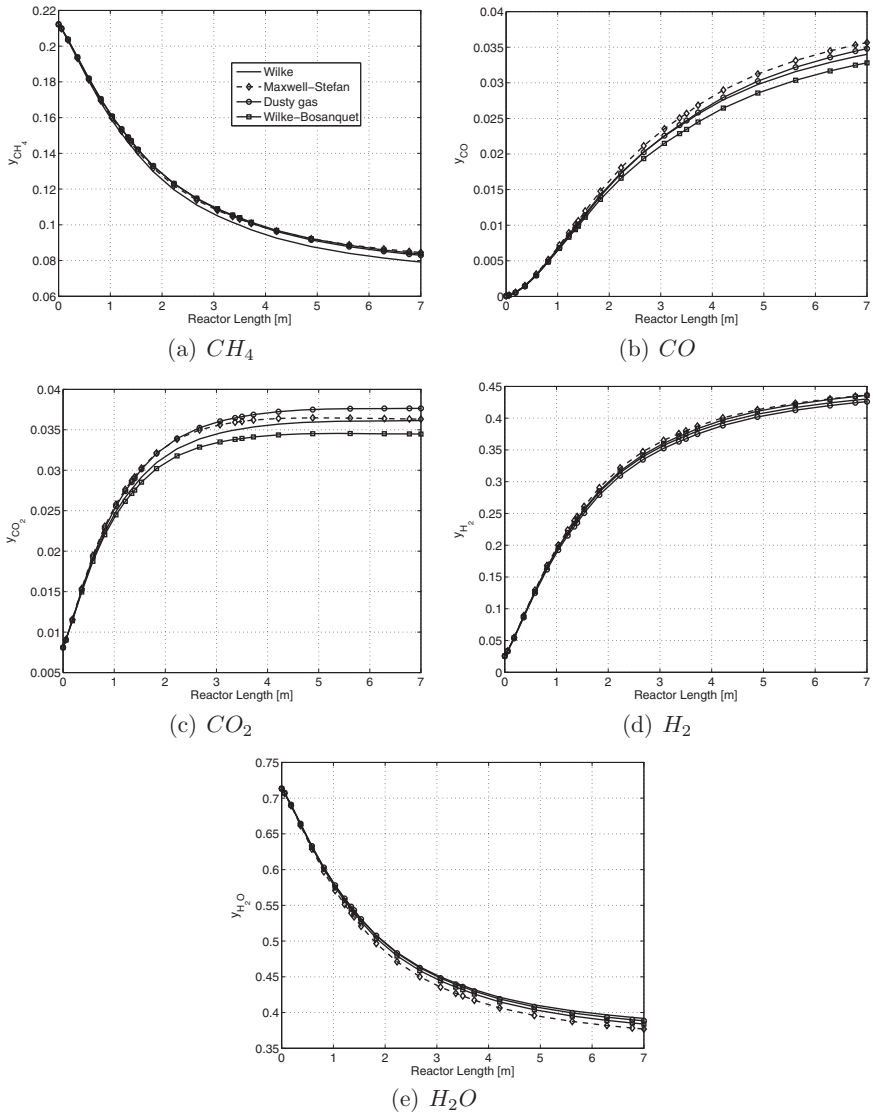

Figure 8. Mole fraction profiles of different components of the SMR process. Comparasion between the Wilke, Maxwell-Stefan, dusty gas, and Wilke-Bosanquet models at reactor level.

process at the pellet level at two mean pore diameters, 50 nm and 25 nm. The simulated results show that the rigorous Maxwell-Stefan and the simpler Wilke models are unaffected by the mean pore diameter of the pellet, which is in accordance with theory. On the other hand, Wilke-Bosanquet is a good replacement for the dusty gas model.

Dependent on the mean pore diameter of the catalyst pellet and reactor operating conditions, the Knudsen diffusion effect can be of paramount importance to include in the pellet model to predict accurate conversion on the level of the reactor. For two different pellet pore diameters, i.e., 50 nm and 25 nm, Figure 10 shows significant differences in the mole fraction profiles of the different components for the SMR process along the reactor axis where the diffusion fluxes are described according to the Wilke, Maxwell-Stefan, Wilke-Bosanquet, and dusty gas models. Hence, if Knudsen diffusion is significant on the level of the pellet, it should be incorporated in the heterogeneous model simulating the whole reactor, because it is most likely that Knudsen diffusion significantly influences the reactor conversion.

Figure 7f shows the temperature profile along the pellet. The temperature variation between the surface and the center of the pellet is less than 1 K. Hence, there is uniform temperature across the pellet. It is found that the velocity across the pellet is zero. The pressure has been calculated from Darcy's law, i.e., Equation (32). So, the pressure gradient is directly proportional to the velocity. As the velocity is zero, there is uniform pressure across the pellet. Furthermore, the diffusive flux is dominant over the convective flux across the pellet. Hence, neglecting the convective flux terms in the temperature equation, pressure equations in the pellet model are reasonable model approximations.

CONCLUSIONS

A numerical simulation was used to investigate the steam methane reforming process by using pseudo-homogeneous, conventional heterogeneous, and simplified heterogeneous reactor models. Three chemical reactions were assumed as the major reactions: two reforming reactions and a water-gas shift reaction. The governing equations and the chemical reactions were

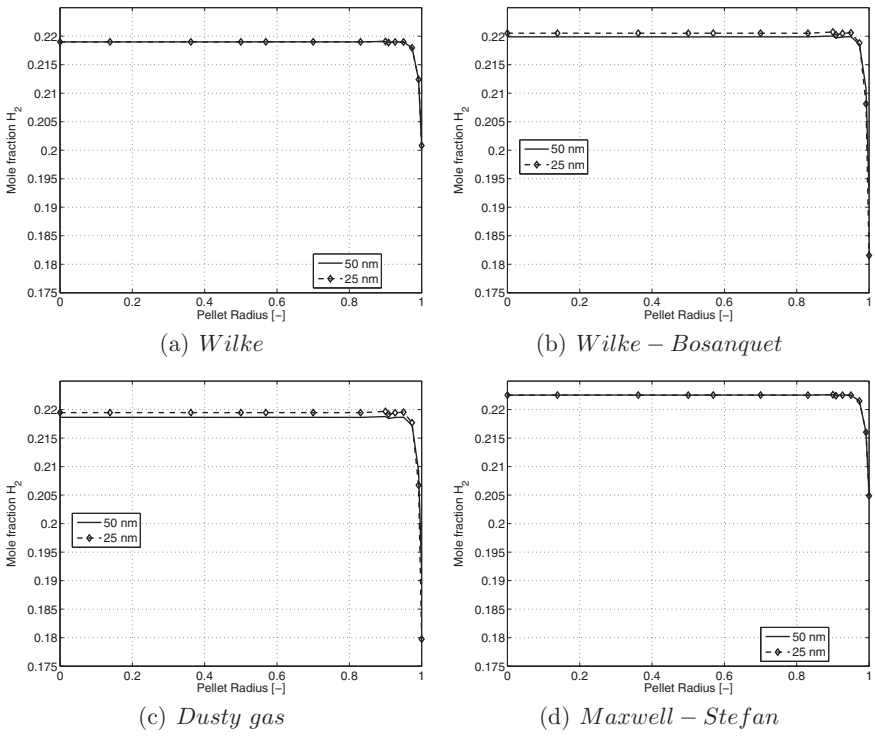

(a) $Wilke$ (b) $Wilke - Bosanquet$

(c) $Dusty\ gas$ (d) $Maxwell - Stefan$

Figure 9. Mole fraction profile of H_2 of the SMR process. Effects of mean pore diameters on pellet level at a distance of 1 m from the entrance of the reactor; Wilke, Maxwell-Stefan, dusty gas, and Wilke-Bosanquet models.

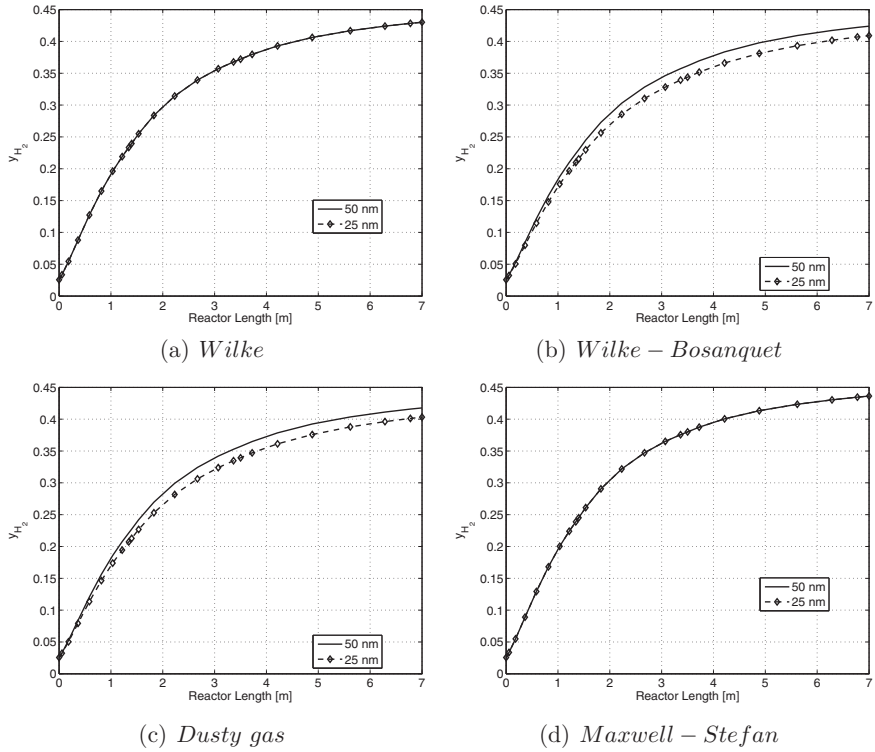

(a) $Wilke$ (b) $Wilke - Bosanquet$

(c) $Dusty\ gas$ (d) $Maxwell - Stefan$

Figure 10. Mole fraction profile of H_2 of the SMR process. Comparison between the Wilke, Maxwell-Stefan, dusty gas, and Wilke-Bosanquet models at reactor level using different pellet pore diameters. Effects of mean pore diameters on pellet level at a distance of 1 m from the entrance of the reactor; Wilke, Maxwell-Stefan, dusty gas, and Wilke-Bosanquet models.

simulated simultaneously in the multiphysical analysis using the least-squares spectral element solution method. For the conventional heterogeneous reactor model, the intra-particle mass diffusion fluxes are described according to Wilke, Maxwell-Stefan, dusty gas, and Wilke-Bosanquet models. The following conclusions were drawn from these calculations.

There is significant deviation between the solid and gas phases of the conventional heterogeneous reactor model. This implies that for the SMR process the heterogeneous reactor model is essential for correct prediction of the output concentration. However, from the detailed analysis of the pseudo-homogeneous, simplified heterogeneous, and conventional heterogeneous reactor models it is found that the maximum difference between the pseudo-homogeneous and the conventional heterogeneous reactor models is 38 %, whereas the maximum difference between the conventional and simplified heterogeneous reactor models is 21 %. As the effectiveness factor of the SMR reactions varies along the reactor length, it is better to use a conventional heterogeneous reactor model for the SMR process. If Knudsen diffusion is significant on the level of the pellet, a combined bulk and Knudsen diffusion model should be adopted to describe the intra-particle diffusion fluxes because Knudsen diffusion significantly influences the reactor conversion. For the reactor operating conditions applied to the SMR process in this study, the Wilke and Wilke-Bosanquet models are good approximations to the rigorous Maxwell-Stefan and dusty gas models, respectively, both on the level of the pellet and to study the impacts of these pellet model closures on the reactor performance.

NOMENCLATURE

A_k	phase cross sectional area (m^2)
a_v	specific surface area of the catalyst pellet (1/m)
Cp	heat capacity of gas mixture (J/kgK)
Cp'_p	heat capacity of solid (J/kgK)
D	binary diffusion coefficient (m^2/s)
D_m	molecular diffusion coefficient (m^2/s)
D^e	effective diffusivity (m^2/s)
$D_{L,j}$	axial diffusivity (m^2/s)
D_k	Knudsen diffusivity (m^2/s)
d_0	average pore diameter (m)
d_p	diameter of catalyst pellet (m)
ΔH	heat of reaction (J/kmol)
h	heat transfer coefficient (W/m^2K)
J	mass diffusion flux (kg/m^2 s)
$\mathbf{J}$	mass diffusion flux (kg/m^2 s)
k	mass transfer coefficient (m/s)
$k_1 * 2.8 * 10^6$	rate constant for Reaction (I) (kmol Pas^2/kg(cat)s)
$k_2 * 27.8$	rate constant for Reaction (II) (kmol Pas/kg(cat)s)
$k_3 * 2.8 * 10^6$	rate constant for Reaction (III) (kmol Pas^2/kg(cat)s)
$K_1 * 10^{10}, K_2, K_3 * 10^{10}$	equilibrium constant for Reactions (I), (II) and (III) (Pas^2, [-], Pas^2)
$K_{CO}/10^5, K_{H_2}/10^5, K_{CH_4}/10^5, K_{H_2O}$	adsorption constant ([Pas^{-1}], [Pas^{-1}], [Pas^{-1}], [-])
L	length of the reactor (m)
M	molecular mass (kg/kmol)
P	pressure (J/m^3)
p	partial pressure (Pa)
Q	heat conductivity flux (W/m^2)
R	gas constant (J/kmol K)
$\mathbf{R}$	reaction rate (kmol/kg(cat) s)
$\mathbf{R}_1/3600$	reaction rate for Reaction (I) (kmol/kg(cat) s)
$\mathbf{R}_2/3600$	reaction rate for Reaction (II) (kmol/kg(cat) s)
$\mathbf{R}_3/3600$	reaction rate for Reaction (III) (kmol/kg(cat) s)
r	radial coordinate (m)
r_p	radius of pellet (m)
t	time (s)
U	heat transfer coefficient (J/m^2 s K)
u	superficial velocity (m/s)
T	temperature (K)
w	species mass fraction
z	reactor axial direction (m)

Greek letters

β_0	friction factor (m^2)
ϵ	porosity
η	internal effectiveness factor
μ	dynamic viscosity (Pa s)
λ	conductivity (W/m K)
ρ	density (kg/m^3)
τ	tortuosity
υ	stoichiometric coefficient of component j in reaction k

Subscript

b	reactor bed
in	initial
g	gas mixture
j	species j
p	pellet
r	radial direction
ref	reference
cat	catalyst

Superscripts

s	solid phase

ACKNOWLEDGEMENTS

The PhD fellowship (Rout, K. R.) financed by the Research Council of Norway through the GASSMAKS program is gratefully appreciated.

REFERENCES

[1] Y. Kalinci, A. Hepbasli, I. Dincer, *Int. J. Hydrogen Energy* **2009**, *34*, 8799.

[2] H. F. Abbas, W. M. A. W. Daud, *Int. J. Hydrogen Energy* **2010**, *35*, 1160.

[3] G. Marban, T. Valdes-Solis, *Int. J. Hydrogen Energy* **2007**, *32*, 1625.

[4] M. Balat, *Int. J. Hydrogen Energy* **2008**, *33*, 4013.

[5] J, Xu, G. F. Froment, *AIChE J.* **1989**, *30*, 88.

[6] J, Xu, G. F. Froment, *AIChE J.* **1989**, *35*, 97.

[7] K. R. Rout, J. Solsvik, A. K. Nayak, H. A. Jakobsen, *Chem. Eng. Sci.* **2011**, *66*, 4111.

[8] G. Pantoleontos, E. S. Kikkinides, M. C. Georgiadis, *Int. J. Hydrogen Energy* **2012**, *37*, 16346.

[9] H. Lindborg, *Modelling and Simulation of reactive two-phase flows in fluidized beds*, PhD thesis, Norwegian University of Science and Technology, Trondheim **2008**.

[10] K. R. Rout, H. A. Jakobsen, *Fuel Process. Technol.* **2012**, *99*, 13.

[11] J. N. Armor, *Appl. Catal., A* **1999**, *176*, 159.

[12] G. F. Froment, K. B. Bischoff, *Chemical Reactor Analysis and Design*, 2nd edition, John Wiley & Sons, Hoboken, NJ **1990**.

[13] H. S. Fogler, *Elements of Chemical Reaction Engineering*, 3rd edition, Prentice Hall, Upper Saddle River, NJ **1999**.

[14] H. A. Jakobsen, *Chemical Reactor Modelling: Multiphase Reactive Flows*, 1st edition, Springer- Verlag Berlin Heidelberg **2008**.

[15] E. N. Fuller, P. D. Schettler, J. C. Giddings, *Ind. Eng. Chem. Res.* **1996**, *58*, 18.

[16] N. Rezaie, A. Jahanmiri, B. Moghtaderi, M. R. Rahimpour, *Chem. Eng. Process* **2005**, *44*, 911.

[17] F. Manenti, C. Silvia, M. Restelli, *Chem. Eng. Sci.* **2011**, *66*, 152.

[18] R. Krishna, J. A. Wesselingh, *Chem. Eng. Sci.* **1996**, *52*, 861.

[19] J. C. Maxwell, *Philos. Trans. R. Soc. Lond.* **1866** *157*, 49.

[20] J. Stefan, *Uber das Gleichgewicht und die Bewegung insbesondere die Diffusion von Gasgemengen*, Sitzungsberichte der Kaiserlichen Akademie der Wissenschaften Wien, 2te Abteilung a, **1871** *63*, 63.

[21] R. Taylor, R. Krishna, *Multicomponent Mass Transfer*, John Wiley & Sons, New York **1993**.

[22] R. Jackson, "Transport in porous catalyst," S. W. Churchill, Ed., *Chemical Engineering Monographs, Volume 4*, Elsevier, Amsterdam **1997**.

[23] E. A. Mason, A. P. Malinauskas, *Gas transport in porous media: The dusty gas model*, Elsevier, New York **1983**.

[24] C. H. Bosanquet, British TA Report BR-507 **1944**.

[25] S. S. E. H. Elnashaie, M. E. E. Abashar, *Chem. Eng. Process.* **1993**, *32*, 177.

[26] A. Burghardt, J. Aerts, *Chem. Eng. Process.* **1988**, *23*, 77.

[27] G. H. Graaf, H. Scholtens, E. J. Stamhuis, A. A. C. M. Beenackers, *Chem. Eng. Sci.* **1990**, *45*, 773.

[28] T. Salmi, J. Warna, *Comput. Chem. Eng.* **1991**, *15*, 715.

[29] S. S. E. H. Elnashaie, M. A. Soliman, M. E. Abashar, *Mathematical and Computer Modelling* **1992**, *16*, 41.

[30] A. M. De Groote, G. F. Froment, T. Kobylinski, *Can. J. Chem. Eng.* **1996**, *74*, 735.

[31] H. M. Wesenberg, *Gas heated steam reformer modelling*, PhD thesis, Norwegian University of Science and Technology, Trondheim **2006**.

[32] E. L. G. Oliveira, C. A. Grande, A. E. Rodrigues, *Can. J. Chem. Eng.* **2009**, *87*, 945.

[33] M. J. Stutz, N. Hotz, D. Poulikakos, *Chem. Eng. Sci.* **2006**, *61*, 4027.

[34] D. R. Parisi, M. A. Laborde, *Comput. Chem. Eng.* **2001**, *25*, 1241.

[35] A. E. Lutz, R. W. Bradshaw, J. O. Keller, D. E. Witner, *Int. J. Hydrogen Energy* **2003**, *28*, 159.

[36] E. Jannelli, M. Minutillo, E. Galloni, *J. Fuel Cell Sci. Tech* **2007**, *4*, 435.

[37] D. D. Davieau, P. A. Erickson, *Int. J. Hydrogen Energy* **2007**, *32*, 1192.

[38] K. Kochloefl, "Steam reforming," G. Ertl, H. Knozinger, J. Weitkamp, Eds., *Handbook of heterogeneous catalysis*, VCH, Weinheim **1997**.

[39] M. F. Edwards, J. F. Richardson, *Chem. Eng. Sci.* **1968**, *23*, 109.

[40] R. B. Bird, W. E. Stewart, E. N. Lightfoot, *Transport Phenomena*, 2nd edition, John Wiley & Sons, New York **2002**.

[41] B. E. Poling, J. M. Prausnitz, J. P. O'Connel, *The Properties of Gases and Liquids*, 5th edition, McGraw-Hill, New York **2001**.

[42] S. Ergun, *Chem. Eng. Proc.* **1952**, *48*, 89.

[43] S. Yagi, D. Kunii, N. Wakao, *AIChE J.* **1960**, *6*, 543.

[44] A. G. Dixon, *Can. J. Chem. Eng.* **1988**, *66*, 705.

[45] E. A. Foumeny, H. A. Moallemi, C. McGreavy, J. A. A. Castro, *Can. J. Chem. Eng.* **1991**, *69*, 1010.

[46] H. A. Jakobsen, H. Lindborg, V. Handeland, *Comput. Chem. Eng.* **2001**, *26*, 333.

[47] N. Wakao, T. Funazkri, *Chem. Eng. Sci.* **1978**, *33*, 1375.

[48] C. L. Yaws, *Chemical Properties Handbook*, McGraw-Hill, New York **1999**.

[49] T. P. Coffee, J. M. Heimerl, *Combust. Flame* **1981**, *43*, 273.

[50] R. Krishna, *Chem. Eng. Sci.* **1992**, *48*, 845.

[51] C. J. Geankoplis, *Transport Processes and Unit Operations*, 3rd edition, Prentice-Hall International Editions, Upper Saddle River, NJ **1993**.

[52] W. W. Akers, D. P. Camp, *AIChE J.* **1955**, *1*, 471.

[53] D. W. Allen, E. R. Gerhard, M. R. Likins, *Ind. Eng. Chem. Process Des. Dev.* **1975**, *14*, 256.

[54] K. Hou, R. Hughes, *Chem. Eng. J.* **2001**, *82*, 311.

[55] C. Hirsch, *Numerical computation of internal and external flows. Volume I: Fundamentals of numerical discretization*, John Wiley & Sons, Chichester **1988**.

[56] J. H. Ferziger, M. Peric, *Computational methods for fluid dynamics*, Springer, Berlin **1996**.

[57] G. D. Smith, *Numerical solution of partial differential equations: Finite difference methods*, 3rd edition, Clarendon Press, Oxford **1985**.

[58] W. E. Schiesser, *The numerical method of lines: Integration of partial differtial equations*, Academic Press, San Diego **1991**.

[59] H. K. Versteeg, W. Malalasekera, *An Introduction to Computational Fluid Dynamics: The Finite Volume Method*, Longman, Harlow **1995**.

[60] B. A. Finlayson, *The method of weighted residuals and variational principles: Mathematics in science and engineering, Vol. 87*, Academic Press, New York **1972**.

[61] F. Sporleder, C. A. Dorao, H. A. Jakobsen, *Chem. Eng. Sci.* **2010**, *65*, 5146.

[62] M. O. Deville, P. F. Fischer, E. H. Mund, *High order methods for incompressible fluid flow*, Cambridge University Press, Cambridge **2002**.

[63] G. E. M. Karniadakis, *Spectral/hp element methods for CFD*. Oxford University Press, New York **1999**.

[64] T. J. R. Hughes, *The finite element method: Linear static and dynamic finite element analysis*, Prentice-Hall, Englewood Cliffs, NJ **1987**.

[65] J. Donea, A. Huerta, *Finite element methods for flow problems*, John Wiley & Sons, Chichester **2003**.

[66] C. Canuto, A. Quarteroni, M. Y. Hussaini, T. Zang, *Spectral methods in fluid mechanics*, Springer-Verlag, New York **1988**.

[67] K. R. Rout, H. A. Jakobsen, *Can. J. Chem. Eng.* **2012**, *91*, 1547.

[68] J. C. De Deken, E. F. Devos, G. F. Froment, *ACS Symposium Series 196-Chemical Reaction Engineering* **1982**, 181.

[69] M. N. Pedernera, J. Pina, D. O. Borio, V. Bucala, *Chem. Eng. J.* **2003**, *94*, 29.

Manuscript received August 27, 2013; revised manuscript received May 5, 2014; accepted for publication May 21, 2014.